Program Digest, 2019 IEEE International Ultrasonics Symposium (IUS)
Glasgow, Scotland, October 6-9, 2019

Simultaneous evalulation of contrast pulse sequences for ultrafast contrast-enhanced ultrasound imaging

Katherine Brown, Kenneth Hoyt *

Department of Bioengineering, University of Texas at Dallas, Richardson, TX, USA
* kenneth.hoyt@utdallas.edu

***Abstract*—The introduction of programmable platforms with plane wave ultrasound (US) transmissions has enabled implementation of various pulsed waveform types at very high frame rates. This study simultaneously evaluated contrast pulse sequences (CPS) employing different amplitude modulation and pulse inversion (AMPI) US imaging schemes. The overarching objective was to improve the contrast-to-tissue ratio (CTR) during ultrafast contrast-enhanced US (CEUS) imaging. Imaging was performed *in vitro* in a tissue-mimicking phantom using a Vantage 256 research scanner (Verasonics Inc). After administration, microbubble (MB) contrast agent disruption was minimized at a frame rate of 300 Hz by using a low mechanical index (MI) acoustic output. A set of basis pulses for transducer transmission was implemented and combined post-acquisition to form various AMPI compositions. Comparisons of different CPS was based on CTR measurements relative to conventional B-mode US images. Simultaneous evaluation reduces variability and allows the use of repeated measures for statistical analysis. A 2-fold improvement in CTR of AMPI compared to B-mode US imaging was found with a flexible transducer waveform implementation of three different length AMPI sequences and one AM sequence. These CPS results are applicable to ultrafast plane wave based CEUS imaging. The developed method is also generalizable to the evaluation of other custom US pulsing strategies.**

Keywords—contrast-enhanced ultrasound, microbubbles, plane wave imaging, ultrasound

I. INTRODUCTION

The emergence of plane wave imaging on programmable ultrasound (US) platforms has enabled ultrafast imaging modes. When coupled with graphics processor units (GPUs), these platforms are able to implement real-time US imaging in both 2-dimensional (2D) and 3-dimensional (3D) space and to improve the field-of-view (FOV), sensitivity and resolution. Ultrafast contrast-enhanced US (CEUS) imaging, as well as the newer super-resolution ultrasound imaging (SR-US) technique, allow visualization of microvessels and the ability to monitor the changes that are present in the progression of cancer, diabetes, and many other diseases [1]–[5]. Doppler US imaging has been shown to improve performance over focused US at high and low blood flow rates [6], [7]. Recent advances with CEUS systems have enabled 3D visualization of blood flow and tissue motion in volume space [8]–[11].

This study was supported by National Institutes of Health (NIH) grants K25EB017222, R01EB025841, and Cancer Prevention Research Institute of Texas (CPRIT) grant RP180670.

The ultrafast frame rates afforded by plane wave US imaging is essential to improving the performance of tissue decluttering techniques and SR-US in microvascular imaging. Angular compounding is used in plane wave imaging to reduce noise by coherently summing received echoes from waves transmitted at multiple angles. To achieve high frame rates, the amount of angular compounding is limited, thus reducing the contrast-to-tissue ratio (CTR). Furthermore, contrast agent destruction during CEUS imaging should be minimized to help improve the accuracy and robustness of any quantitative analysis of the US image sequences [12]. While a lower acoustic output (mechanical index, MI) reduces the likelihood of any MB destruction, use of a lower MI will also lower the nonlinear response of the MB and also decrease image CTR [13], [14]. There is tradeoff in raising the MI; while it increases the nonlinear backscattered US signal, it also stochastically increases the probability of MB destruction. In addition, the slow blood flow rates present in the microvasculature networks (< 10 cm/sec) reduce CTR due to slow replenishment of MBs in the vessels following any destruction. The combination of low angular compounding, low MI, and low flow rates presents a challenge to obtaining a high CTR during ultrafast plane wave CEUS imaging of microvasculature networks such as associated with tumor angiogenesis.

Various nonlinear methods to enhance the contrast of MBs in plane wave imaging have been explored [14], [15]. One of the earliest nonlinear techniques was pulse inversion (PI) imaging, which employs 2 pulses with opposite phase. The echoes from the 2 pulses are combined, cancelling the linear portion of the response. This technique was extended with the incorporation of amplitude modulation (AM) to pulse inversion, resulting in AM with pulse inversion (AMPI). AMPI retains more energy at the fundamental frequency and improves the CTR. Based on either PI, AM, or AMPI, studies of these contrast pulse sequences (CPS) have generally shown the superiority of AMPI [16]–[18].

The goal of this study is to evaluate the selection of CPS on image CTR with ultrafast US imaging. Few CPS studies have been performed with ultrafast US imaging using plane wave transmissions, and none to our knowledge used a simultaneous method of comparison. The unique aspect of this study is the methodology underlying the simultaneous method of comparison of pulse sequences that is made possible by the recent introduction of programmable US platforms. A set of basis pulses was selected and programmed for sequential

transmission. A variety of combinations of these pulses were summed to create different frame sequences from the identical pulses. Alternatively, a comparison of pulse sequences could have been made in separate experiments, but this would have introduced additional experimental variation.

II. MATERIALS AND METHODS

Lipid encapsulated perfluorocarbon MBs were prepared using established methods [19]. Imaging was performed with an US research scanner (Vantage 256, Verasonics Inc., Kirkland, WA) equipped with a L11-4v linear array transducer at a transmit frequency of 6.25 MHz. Scripts were customized to program the US hardware with the desired pulse sequence then combined to create the CPSs explored in this study. Time gain compensation (TGC) settings were identical for all measurements. A minimal amount of plane wave angular compounding was implemented (3 angles at -5, 0, and 5º). The interval between transmissions was 160 μs to allow for full depth penetration, and the frame rate was 300 Hz. In order to obtain a time average of CTR, 300 frames were captured over a 1-min interval in groups of 30 frames equally spaced in time. Radio frequency (RF) data was captured for post-processing.

Acoustic properties for the Vantage 256 system with the L11-4v linear array transducer were measured in a water bath with a hydrophone system (Aims III, Onda Corp., Sunnyvale, CA). A derated MI was computed based on an attenuation coefficient of 0.3 dB/MHz/cm. Basis pulse waveforms were recorded for offline analysis. A set of 5 basis pulses which can be combined to form the 4 studied CPS candidates and the method of combining them is depicted in Fig. 1. The 5 basis pulses were: +0.5, -1, +1, -0.5, +0.5. A "1" indicates the normalized voltage amplitude, and "0.5" indicates half the normalized voltage amplitude, "-" sign indicates pulse inversion, and "+" sign indicates no inversion. The studied sequences of AM and AMPI have a length of 2 pulses (AMPI-2, AM-2), 3 pulses (AMPI-3) or 4 pulses (AMPI-4).

The method for AM was a direct programming of the amplitude level of the pulse in the Verasonics US system. The pulse length for each basis pulse was programmed for a single cycle. Raw RF data was linearly combined with custom MATLAB processing software (MathWorks Inc., Natick, MA) to form each CPS sequence. The combined data for CPS sequences was then processed to form images with Verasonics proprietary code. The final step was a post-processing step using MATLAB to calculate a CTR from the US images constructed.

In vitro characterization was conducted in a vascular flow phantom (Model 524, ATS Labs Bridgeport, CT) with a MB contrast agent flowing through a 2-mm tube (depth of 15 mm) embedded in a tissue-mimicking material. A 2.5 x 10^5 MB/mL solution was pumped (Model 77200-60, Cole-Palmer, Vernon Hills, IL) from a stirred chamber. A flow rate of 10 mL/min was chosen to model microvasculature flow of about 5 cm/sec. For each experiment, data was taken at the peak intensity of the wash-in, as determined experimentally by taking the average intensity of thirty frames every 10 sec over 5 min. The experiment was repeated three times at five levels of MI between 0.1 and 0.5 with a fresh bolus of MB.

For CTR analysis, an average was computed for each CPS candidate and group of 30 frames. From the resulting image, a CTR was computed as:

$$CTR = \frac{\mu_{bubble}}{\mu_{tissue}} \quad (1)$$

where μ_{bubble} is the mean intensity within the region-of-interest (ROI) of the contrast agent, and μ_{tissue} is the mean intensity of the ROI for the tissue. The contrast agent ROI is within the 2-mm tubing, and the tissue ROI is of an equal pixel area composed of two regions, one immediately below and one above the tubing. For comparison purposes, a CTR ratio capturing the improvement of the nonlinear contrast pulse sequencing with the

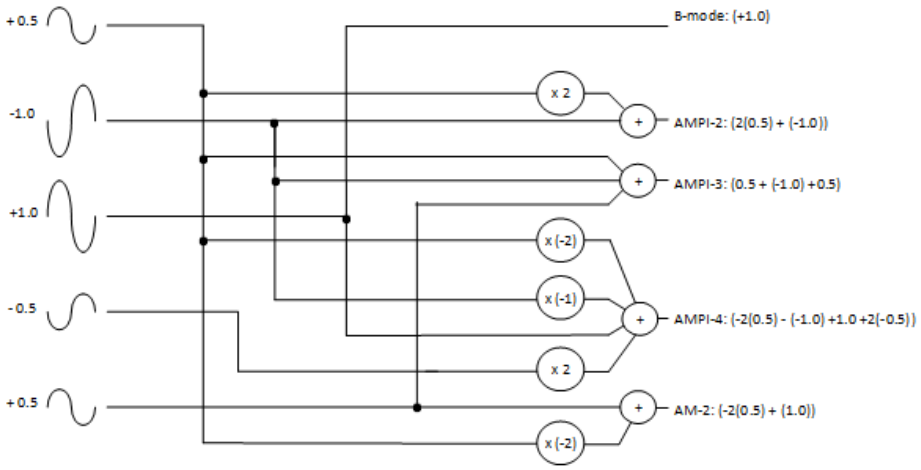

Fig. 1: Composition diagram of contrast pulse sequences (CPS) showing the combination of the 5 basis pulses at the top to create the studied sequences of amplitude modulation (AM) and AM with pulse inversion (AMPI) with a length of 2 pulses (AMPI-2, AM-2), 3 pulses (AMPI-3) or 4 pulses (AMPI-4).

corresponding B-mode US image, captured simultaneously, was computed as:

$$CTR_{ratio} = \frac{CTR_{CPS}}{CTR_{B-mode}} \quad (2)$$

All data was summarized as mean data ± standard deviation. The variance in multiple measurements was viewed as an indicator of reproducibility. Repeated measures ANOVA was used to evaluate the different CPS compositions as they were produced simultaneously. Any p-value less than 0.05 was considered statistically significant.

III. RESULTS

The four unique basis pulses were measured with a hydrophone in a water tank and the digitized waveforms are shown in Fig. 2a. The hydrophone measurements were used to ensure that the spectrum of the half pulse programmed was approximately half the height as the full pulse. The ultrasound platform internal timing of receiver cannot be observed. Thus, the alignment of data waveforms sampled by the hydrophone system can only be approximated to that of the alignment of received data within the ultrasound platform. The basis pulses are closely matched in shape and zero crossings, yet some difference in the slope of the rising and falling edges is apparent.

The linear combinations of basis pulses forming each CPS composition in Fig. 2b reveals the residual values from imperfect cancellation of the positive and negative pulses and imperfections in amplitude scaling. With only an approximate alignment of waveforms, this summation is also an estimate. Shifts of the waveforms from the positions shown in Fig. 2a resulted in larger residual values after summation.

In Fig. 3, the mean contrast level for each CPS composition is shown for MI levels between 0.1 and 0.5, with peak negative pressures from 391 kPa to 1.0 MPa. Overall, the highest CTR ratio value was a 2-fold improvement obtained for AMPI-4 and AMPI-3 CPSs compared to B-mode. For each CPS composition, the trend of CTR ratio with MI values followed a similar shape. CTR ratio slightly increased with increasing MI from an MI of 0.1, peaking at an MI of 0.2 to 0.3, and then decreasing with further increases of MI. The largest CTR values are obtained with an MI value of 0.2 for AMPI-2, AMPI-3, and AMPI-4, while the largest CTR value is obtained with an MI value of 0.3 for AM-2. These trends were small in percentage terms and in relation to the standard deviations of the measurement. Statistically, the ANOVA results showed the CPS composition (as it affects CTR ratio) is significant ($p < 0.001$).

Disruption of the MBs was observed during the study at all MI levels. When US transmission was resumed after a period of time without transmissions while data was collected, the images were at first noticeably brighter within the channel containing MB, and then dimmed over a few seconds before coming to a constant level. A similar change in image intensity was also observed if the pump speed was lowered by a factor of 10, (e.g. from 10 to 1 mL/min). As this effect could be repeated during a trial with a single MB bolus, it was understood to be MB destruction with US exposure rather than dissolution over time.

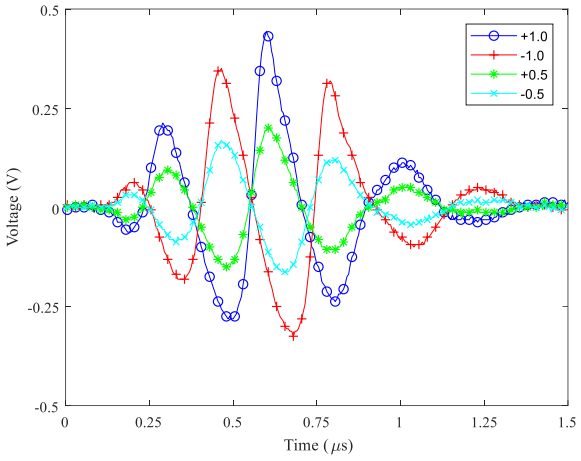

(a)

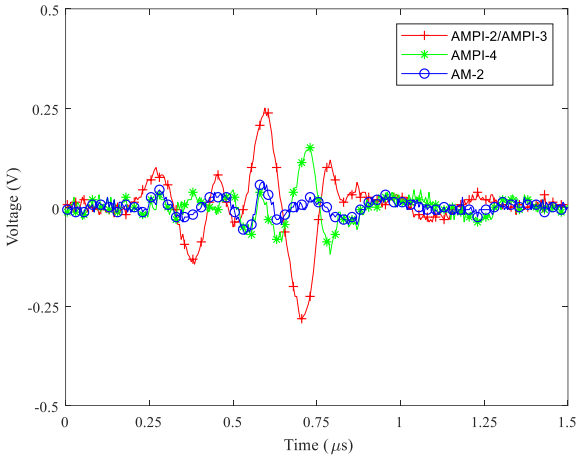

(b)

Fig. 2: Waveforms for (a) 4 basis pulses at 6.25 MHz: +1.0, -1.0, +0.5, -0.5. (b) CPS compositions from linear combination of basis pulses: AMPI-2/AMPI-3, AMPI-4, AM-2.

IV. DISCUSSION

Prior studies of contrast pulses have concluded that up to 20 dB improvement may be expected under certain conditions. Phillips found the highest specificity *in vitro* with a 3-pulse AMPI sequence at MI values below 0.3, and with a 4-pulse AMPI sequence at MI values above 0.3, at 1.7 MHz with a stationary contrast agent [17]. Eckersley et al. studied 2-pulse sequences of AM, PI and AMPI in a 2 MHz *in vitro* study using two single element transducers at 0.1 MI [16]. They found the highest contrast was using 2-pulse AMPI with an 18 ± 2 dB improvement compared to the echoes from a linear scatterer. Needles et al. evaluated PI, AM, and AMPI both *in vivo* and *in vitro* at a flow rate of 30 mm/sec and 18 - 24 MHz, and demonstrated a 13 - 15 dB improvement in CTR of AM/AMPI compared to fundamental imaging [18].

The results of this study at low MI levels are consistent with the results by others in that the longer 3-pulse and 4-pulse AMPI

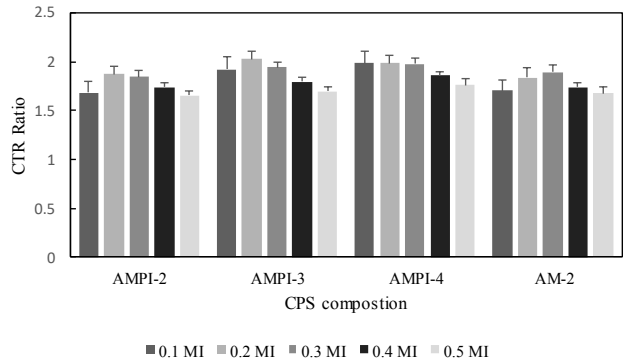

Fig. 3: Comparison of 4 CPS compositions at MI values from 0.1 to 0.5 with a slow flow rate reveals slight differences in contrast with pulse composition and slight superiority of the longer pulse sequences: AMPI-3 with three pulses and AMPI-4 with four pulses at an MI of 0.2.

sequences have the highest CTR. Considering the nonlinear backscattered US signal from a MB as a power series expansion, this would be explained by the higher content of second and third harmonics of these compositions [17]. Longer pulse sequences would benefit from improved SNR with averaging of 3 to 4 pulses. In addition, pulse inversion enhances the nonlinear response of MBs, and AM compositions would be expected to perform less well than similar length AMPI compositions. Overall, these expectations were borne out by the results. AMPI-3 shows the highest CTR ratio, closely followed by AMPI-4, with AMPI-2 and AM-2 displaying lower CTR ratios.

This study revealed a tradeoff of higher MI levels with greater echogenicity of the MB's nonlinear response but with more disruption. This led to an intermediate yet low value of MI showing the highest CTR ratio. The overall differences in the CTR ratios of the study were modest, with the difference in highest CTR ratio at 2.1 for AMPI-3 at an MI of 0.2, only 6.5% better than the highest CTR ratio for AM-2 of 1.9 at MI of 0.3. This study also revealed a smaller improvement in CTR than other studies, which is thought to be primarily the result of the experimental conditions and choice of reference for comparison. Three angles were compounded in the plane wave images in this study, considerably less than a typical 15 – 63. This limited the intensity of the coherently summed echoes. A slow flow rate increased the time MBs were subject to US energy, contributing to their dissolution. An extended time for replenishment of fresh MB in the vessel contributed to a reduced CTR. This study compared plane wave CPS imaging to plane wave B-mode US imaging. The nonlinear echo of a MB present in B-mode US imaging would be expected to be stronger than one from the linear US scatterer used as a reference, reducing relative CTR. In addition, the imperfect pulse cancellation for the CPSs may be attributable to the hardware pulser circuit of the US system.

V. CONCLUSION

The results of these simultaneous experiments show that CPS used during ultrafast CEUS imaging can improve the CTR ratio by 2-fold over conventional B-mode US. Shorter sequences (e.g. 2 transmit pulses) performed only slightly worse than longer sequences (e.g. 3 or 4 transmit pulses) but enable marginally higher frame rates. If an US platform does not have an effective pulse inversion, amplitude modulation alone with a pulse sequence such as AM-2, may be considered. Of particular note, the higher US frame rates enabled with a 2-pulse sequence may be advantageous to maximizing the volume scan rate for ultrafast 3D CEUS imaging. In addition, the programmable US platform enables greater flexibility in experimentation. This allows simultaneous experiments and is generally translatable to the exploration of pulse sequences offering a further reduction in variation and the associated greater statistical power.

REFERENCES

[1] C. Errico *et al.*, "Ultrafast ultrasound localization microscopy for deep super-resolution vascular imaging," *Nature*, vol. 527, no. 7579, p. 499, 2015.
[2] D. Ghosh *et al.*, "Monitoring early tumor response to vascular targeted therapy using super-resolution ultrasound imaging," *Proc IEEE Ultrason Symp*, pp. 1–4, 2017.
[3] D. Ghosh *et al.*, "Super-resolution ultrasound imaging of the microvasculature in skeletal muscle: A new tool in diabetes research," *Proc IEEE Ultrason Symp*, pp. 1–4, 2017.
[4] K. Tanigaki *et al.*, "Hyposialylated IgG activates endothelial IgG receptor FcγRIIB to promote obesity-induced insulin resistance," *J Clin Invest*, vol. 128, no. 1, pp. 309–322, 2018.
[5] D. Ghosh *et al.*, "Super-resolution ultrasound imaging of skeletal muscle microvascular dysfunction in an animal model of type 2 diabetes," *J Ultrasound Med*, published online 2019.
[6] J. Bercoff *et al.*, "Ultrafast compound Doppler imaging: Providing full blood flow characterization," *IEEE Trans Ultrason Ferroelectr Freq Control*, vol. 58, no. 1, pp. 134–147, 2011.
[7] E. Macé *et al.*, "Functional ultrasound imaging of the brain," *Nat Methods*, vol. 8, no. 8, pp. 662–664, 2011.
[8] J. Provost *et al.*, "3D ultrafast ultrasound imaging in vivo," *Phys Med Biol*, vol. 59, no. 19, pp. 1–13, 2014.
[9] M. Mahoney *et al.*, "Volumetric contrast-enhanced ultrasound imaging of renal perfusion," *J Ultrasound Med*, vol. 33, no. 8, pp. 1427–1437, 2014.
[10] K. Hoyt, A. Sorace, and R. Saini, "Quantitative mapping of tumor vascularity using volumetric contrast-enhanced ultrasound," *Invest Radiol*, vol. 47, no. 3, pp. 167–174, 2012.
[11] K. Hoyt, A. Sorace, and R. Saini, "Volumetric contrast-enhanced ultrasound imaging to assess early response to apoptosis-inducing anti-death receptor 5 antibody therapy in a breast cancer animal model," *J Ultrasound Med*, vol. 31, no. 11, pp. 1759–1766, 2012.
[12] R. Saini and K. Hoyt, "Recent developments in dynamic contrast-enhanced ultrasound imaging of tumor angiogenesis," *Imaging Med*, vol. 6, no. 1, pp. 41–52, 2014.
[13] N. de Jong *et al.*, "Ultrasonic characterization of ultrasound contrast agents," *Med Biol Eng Comput*, vol. 47, no. 8, pp. 861–873, Aug. 2009.
[14] J. Viti *et al.*, "Detection of contrast agents: Plane wave versus focused transmission," *IEEE Trans Ultrason Ferroelectr Freq Control*, vol. 63, no. 2, pp. 203–211, 2016.
[15] O. Couture, M. Fink, and M. Tanter, "Ultrasound contrast plane wave imaging," *IEEE Trans Ultrason Ferroelectr Freq Control*, vol. 59, no. 12, pp. 2676–2683, 2012.
[16] R. J. Eckersley, C. T. Chin, and P. N. Burns, "Optimising phase and amplitude modulation schemes for imaging microbubble contrast agents at low acoustic power," *Ultrasound Med Biol*, vol. 31, no. 2, pp. 213–219, 2005.
[17] P. Phillips and E. Gardner, "Contrast-agent detection and quantification," *Eur Radiol*, vol. 14 Suppl 8, pp. 4–10, 2004.
[18] A. Needles *et al.*, "Nonlinear contrast imaging with an array-based micro-ultrasound system," *Ultrasound Med Biol*, vol. 36, no. 12, pp. 2097–2106, 2010.
[19] S. Sirsi and M. Borden, "Microbubble compositions, properties and biomedical applications," *Bubble Sci Eng Technol*, vol. 1, no. 1–2, pp. 3–17, 2009.